

Characteristics of sisal-epoxy composite boards with sodium chloride-treated fibers at different treatment temperatures

Tamaryska Setyayunita¹, Heru Suryanto^{1*}, Aminnudin Aminnudin¹, Azlin Fazlina Osman², and Uun Yanuhar³


¹ Department of Mechanical and Industrial Engineering, Faculty of Engineering, Universitas Negeri Malang, **Indonesia**

² Faculty of Chemical Engineering & Technology, Universiti Malaysia Perlis, **Malaysia**

³ Department of Aquatic Resources Management, Universitas Brawijaya, **Indonesia**

* Corresponding Author: heru.suryanto.ft@um.ac.id

Received: 20 April 2025; *Revised:* 02 June 2025; *Accepted:* 03 June 2025

 Cite this <https://doi.org/10.24036/teknomekanik.v8i1.35572>

Abstract: The growing environmental concerns associated with synthetic fibers have led to the increased adoption of bio-fibers as reinforcements in polymer composites. Sodium chloride (NaCl) is explored as a fiber treatment agent to enhance the adhesion between fibers and the matrix. The study aims to evaluate the effects of NaCl treatment on the characteristics of sisal fiber-epoxy composite boards. A completely randomized design was applied with three factors: treatment temperature (25°C and 100°C), NaCl concentration (1, 3, and 5 wt%), and composite board density (0.40, 0.60, and 0.80 g/cm³). Sisal fibers were soaked in NaCl solutions for one hour, rinsed, dried, and manually blended with epoxy at a ratio of 80:20 wt%. Composite board properties were observed according to the standards of JIS-A-5908, Fourier Transform Infrared Spectroscopy (FTIR), and Scanning Electron Microscopy (SEM). Results indicated that increasing the NaCl concentration and treatment temperature significantly improved the properties of the composite board. The optimal parameters (5wt% NaCl, 100°C, 0.80g/cm³) yielded a modulus of elasticity of 4.59±0.26 GPa, modulus of rupture of 18.88±0.03 MPa, and internal bond strength of 3.92±0.18 MPa, representing increases of 200.32%, 130.65%, and 218.70%, respectively. Thickness swelling decreased to 2.13±0.43% (48.14%) and water absorption to 8.95±0.05% (32.25%). These findings confirm that NaCl treatment is an eco-friendly method to enhance the mechanical strength and moisture resistance of biofiber composites. It also supports the development of high-performance composite boards.

Keywords: composite boards; mechanical properties; epoxy; NaCl treatment; sisal fiber

1. Introduction

Synthetic polymer is an attractive material due to its properties, such as lightweight and flexibility [1], which can be applied as composite materials [2], [3] for a structural component [4]. However, sustainable alternatives-particularly biofibers-are increasingly recognized as viable replacements for synthetic polymer fibers. Beyond biofibers, natural fillers and nanomaterials (e.g., cellulose) enhance advanced composite functionalities, including antibacterial, mechanical, and sensing properties [5],[6]. Advantages such as low density, biodegradability, renewability, and cost-effectiveness have garnered significant research and industrial interest [7]. Common biofibers (ramie, jute, kenaf, coconut, sisal) serve as primary reinforcements and fillers in polymer composites, improving tensile and flexural strength [8]. Notably, sisal fiber exhibits mechanical performance comparable to synthetic fibers as a potential reinforcement material [9].

Sisal fiber is widely used in commercial applications, including composite boards offering higher strength and lower weight than plywood. Extensive studies have developed sisal composites with various adhesives, including epoxy, emerging as a preferred choice due to its superior performance. As a polymer adhesive, epoxy provides high stiffness, dimensional stability, and chemical resistance. Thus, it is an ideal bonding agent for fiber-reinforced materials [10],[11]. Weak fiber-adhesive adhesion remains a major challenge in biofiber composites, as mechanical properties depend critically on the strength and interfacial bond integrity [12],[13]. Biofibers (hemp, jute, and sisal) contain lignocellulosic biopolymers with abundant hydroxyl groups, conferring polar/hydrophilic characteristics and high-water affinity [14]. Conversely, most polymer matrices are hydrophobic. This incompatibility results in poor interfacial adhesion [15],[16], leading to weakened bonding.

The disparity in surface properties often results in weak fiber-adhesive adhesion, compromising the overall mechanical performance of composite materials. Various chemical treatments and fiber modifications have been explored to enhance compatibility and strengthen the interfacial bonding. Techniques such as esterification [17], NaOH treatment [18], and silane coupling agents [19] have proven effective in enhancing fiber-adhesive interactions, thereby improving the mechanical properties of the composite boards. Therefore, chemical treatment has become a key area of study, driving advancements in the performance and durability of biofiber-reinforced composite boards for diverse applications [20]. However, high-pH materials commonly used for fiber modification can cause damage to production equipment. Neutral-pH alternatives, such as NaCl, offer promise for improving fiber properties without compromising industrial processing or equipment longevity [21]. Physical methods (plasma [22] and ultraviolet radiation [23]) alter surface texture and structural characteristics without chemical changes, while chemical treatments permanently modify fiber cell walls through grafting, bulking, or cross-linking [7].

Studies on the utilization of pure NaCl for biofiber treatment have shown the potential to increase the strength of composite boards. NaCl treatment of kenaf fibers (5%, room temperature) increased mechanical strength and elastic modulus of up to 16.06% and 24.29%, respectively [24]. It also improved the properties of epoxy-adhesive composite boards with an optimal adhesive content of 20% [24] that meet the JIS A 5908 type 8 standard [25], [26]. However, fiber modification at room temperature does not meet JIS A 5908 types 13 and 18. The combined effects of elevated temperatures and varying NaCl concentrations remain unexplored, as do lower densities critical for cost-effective structural performance [27]. While JIS A 5908 defines medium-density boards (0.4–0.9 g/cm³), density effects on NaCl-treated sisal composite boards are underdeveloped. Studies on fiber treatment using NaCl remain limited, and the influence of elevated temperature during the treatment process has not yet been thoroughly investigated. Therefore, this study evaluates the influence of NaCl concentration, modification temperature, and density on the properties of composite board. The analysis includes tensile strength testing, Fourier Transform Infrared Spectroscopy (FTIR), and surface morphology characterization using Scanning Electron Microscopy (SEM) to evaluate the properties of composite boards comprehensively.

2. Material and methods

2.1 Materials

Sisal fiber (*Agave sisalana*) from Blitar District of East Java, Indonesia, was selected as the primary material for this study. Epoxy resin (Diglycidyl Ether of Bisphenol A type) and hardener (aliphatic amine type) purchased from Alfatama, Indonesia, were used as the adhesive binder for fabricating the composite boards. NaCl (99% purity, Sigma-Aldrich, Singapore) was used for fiber treatment.

2.2 Sample preparation

Sample preparation is shown in Figure 1.

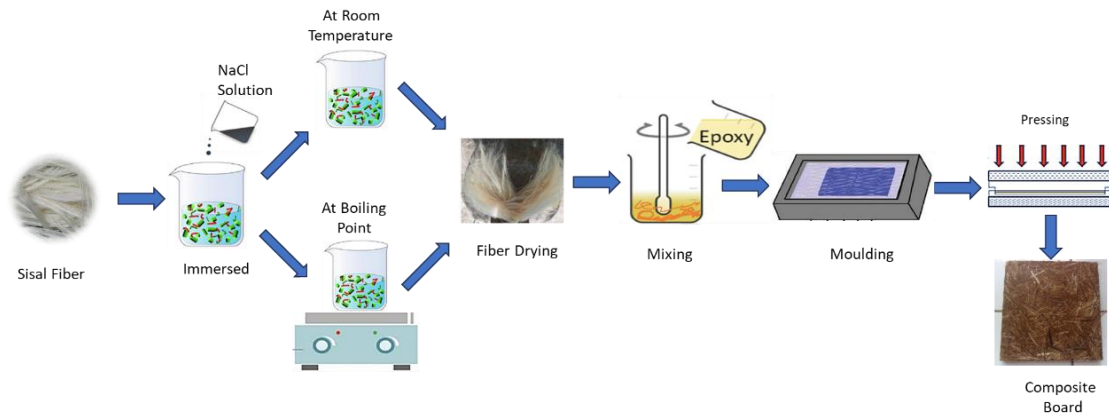


Figure 1. Sample preparation

2.2.1 Sodium chloride treatment

Sisal fibers were air-dried to a moisture content of 13–14% at room temperature and cut to 25 mm lengths. It was immersed in 1 wt%, 3 wt%, and 5 wt% NaCl solution for an hour at room temperature or boiling point (± 100 °C). Fibers were rinsed to pH 7 and dried to complete the treatment. The ratio of fiber to solution was maintained at 1:20 (w/w) throughout the process.

2.2.2 Composite board production

Epoxy and hardener (1:1 g/g) were blended manually with sisal fiber (80% wt). Test samples were fabricated using a mat with dimensions of 250 mm \times 250 mm \times 150 mm. The composite was pressed using a cold pressing machine to achieve a final thickness of 10 mm. Once the samples were prepared, they were trimmed to standard dimensions for testing, with each test being repeated three times. Mean values and standard deviations were then calculated to assess the results. Figure 2 shows the composite board from sisal fiber and epoxy.



Figure 2. Composite board from sisal fiber and epoxy

2.3 Composite board properties

The composite board properties were evaluated following the guidelines of JIS-A-5908 [26]. The properties include internal bonding strength (IB), modulus of elasticity (MOE), modulus of rupture (MOR), water absorption (WA), and thickness swelling (TS). Specimens with dimensions 50 mm \times 50 mm \times 10 mm for IB, TS, and WA testing. Specimens were immersed in water for 24 hours at room temperature to measure TS and WA. Before and after immersion, the thickness and weight

of the specimens were recorded. Meanwhile, specimens with dimensions 200 mm × 50 mm × 10 mm were tested under dry conditions for flexural properties (static three-point bending). The support distance during testing was 150 mm. The rate was set to 10 mm/min with triplicate testing for each treatment. The results presented in the figures included error bars to exhibit the standard deviations of the results. The standard deviation is exhibited by vertical lines displayed on the bars, indicating the variability within the data. Groups showing significant differences ($p < 0.05$) are marked with distinct letters in the graph.

2.4 Functional group analysis

An FTIR Shimadzu IR Prestige-21 spectrometer (Japan) was used to analyze the functional group. Samples were dried (40°C, overnight) to remove all residual moisture content. After drying, the samples were ground into fine powder using a mill machine to ensure uniformity and to facilitate better interaction with the infrared radiation. The spectra were then obtained using the KBr disk method, which involves mixing the sample with potassium bromide (KBr) and pressing it into a flat pellet. Spectra capture 10 scans to increase the accuracy of the results at 16cm⁻¹ resolution for detailed functional groups present in the composite board.

2.5 Surface morphology analysis

SEM Hitachi TM400 (Japan) at a voltage of 15.0 kV was used to examine the surface morphology.

2.6 Data analysis

The one-way ANOVA (analysis of variance) was used to analyze the significant influences of NaCl treatments on composite board properties. The parameters analyzed included physical properties such as TS and WA, as well as mechanical properties including IB, MOE, and MOR.

3. Results and discussion

3.1 Mechanical properties

The MOE and MOR of the treated sisal fiber composite board increased significantly with NaCl treatment (Figure 3). The maximum MOE (4.59 ± 0.26 GPa) and MOR (18.88 ± 0.03 MPa) occurred at 0.80 g/cm³ density with 5 wt% NaCl at the boiling point. Minimum value of MOE (2.30 ± 0.26 GPa) and MOR (6.50 ± 0.03 MPa) occurred at 0.40 g/cm³ density with 1 wt% NaCl at room temperature. Compared to untreated sisal fiber (0.80 g/cm³ density), MOE increased by 130.65% (from 1.99 GPa to 4.59 GPa), and MOR increased by 200.32% (from 6.29 MPa to 18.88 MPa). These findings confirm that NaCl treatment significantly enhances the mechanical properties of sisal fiber composites, with higher concentrations and boiling point yielding the most substantial enhancement.

The trends observed for the MOE and MOR in NaCl-treated sisal fiber composite boards align with the trends in tensile strength and elastic modulus of sisal fiber subjected to various treatment conditions. The 5 wt% NaCl treatment at the boiling point notably increased the elastic modulus and strength of sisal fiber by 76.8% and 48.39%, respectively, compared to fibers without treatment [21]. An increase in the mechanical properties of sisal fibers had a corresponding significant effect on the mechanical properties of the composite boards. The increase in MOE and MOR is due to the adsorption of Na⁺ ions on the fiber's surface. It reduces lignin content by attaching to certain chemical groups, making the fiber surface more compatible with the epoxy and providing a rougher fiber surface. Na⁺ adsorption alters the crystallinity of the fiber and surface topology, enhancing mechanical interlocking with the epoxy matrix. The fiber bonds strongly with

the epoxy, improving the overall strength and durability of the composite. This alteration in the fiber composition strengthens the treated fibers [28]. Therefore, the treated fiber properties of composite boards are more robust since the NaCl treatment significantly enhances the overall performance of biofiber-based composites.

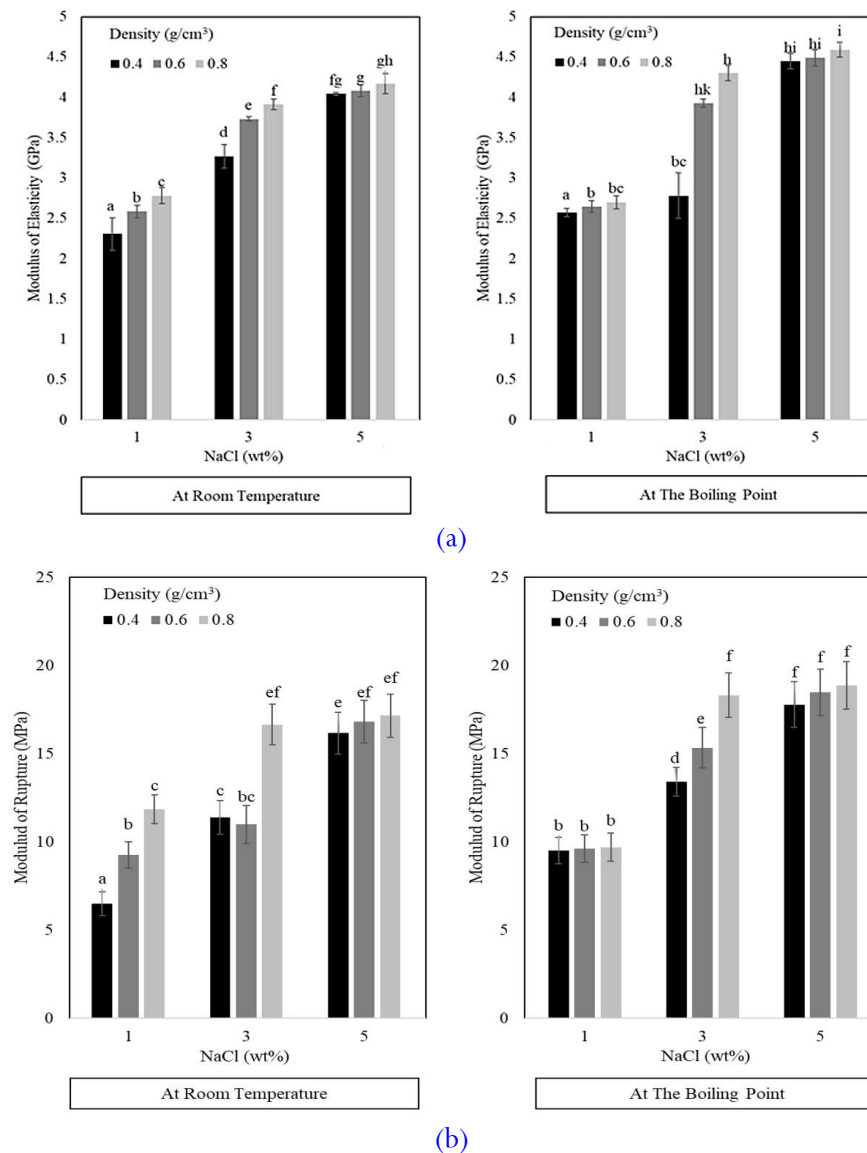


Figure 3. Mechanical properties of NaCl-treated sisal fiber-epoxy composite board: (A) MOE and (B) MOR

The maximum MOR occurred at a density of 0.80 g/cm^3 with 3 wt% NaCl-treated sisal fiber at the boiling point. At higher NaCl concentrations, the MOR did not increase significantly with increasing composite board density. However, overall trends confirm that increased NaCl concentration, temperature, and density enhance the bending strength and IB (Figure 4). The increase in the bending strength of the composite board is supported by the increase in the binding power between the fibers and the adhesive, so that the IB of the board is also stronger [8], [9]. The maximum IB ($3.92 \pm 0.18 \text{ MPa}$) occurred at the boiling point with 0.80 g/cm^3 and 5 wt% NaCl. The minimum IB ($1.26 \pm 0.05 \text{ MPa}$) occurred at room temperature with 0.40 g/cm^3 and 1 wt% NaCl. The NaCl-treated fiber composites consistently exhibited higher IB compared to the untreated fiber composite boards. IB strength increased by 17.76% at 0.40 g/cm^3 (from 1.07 MPa to 1.26 MPa), 47.06% at 0.60 g/cm^3 (from 1.19 MPa to 1.75 MPa), and 218.70% at 0.80 g/cm^3 (from 1.23 MPa to 3.92 MPa).

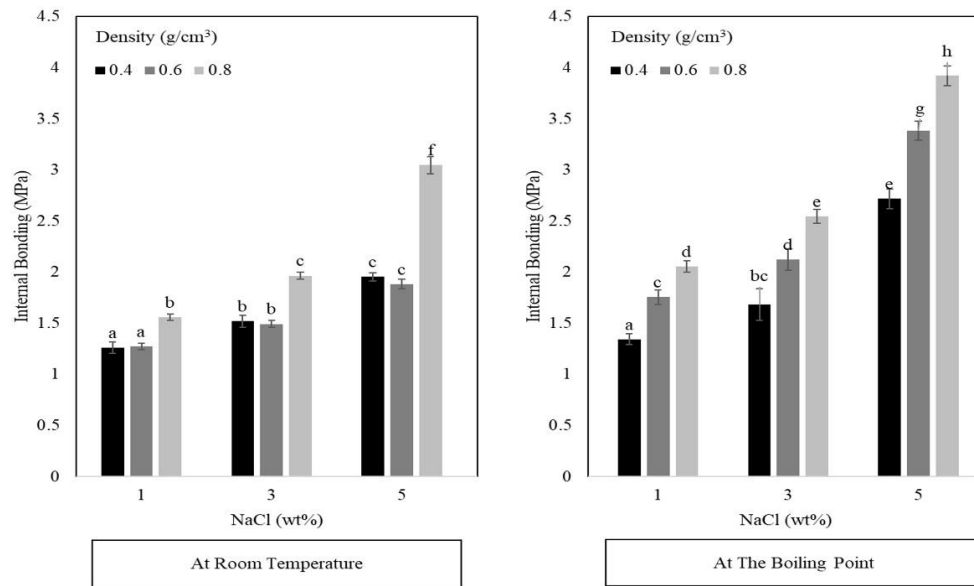


Figure 4. IB of sisal fiber-epoxy composite board with NaCl treatment

These results confirm that NaCl treatment significantly enhances fiber-matrix adhesion. Higher concentrations and boiling points yield the best bonding performance. The removal of impurities and fibrillation enhances bonding strength, resulting in improved epoxy penetration and an increased contact area between the epoxy and substrate [12]. According to a previous study [20], the contact angle of sisal fiber was 124° , which significantly decreased to 76° after being treated with 5 wt% NaCl under boiling conditions. This decrease in contact angle indicated that NaCl treatment enhances the epoxy wettability on treated fibers compared to untreated fibers. The smaller contact angle suggested better adhesive absorption, resulting in more effective coverage of the fiber bundles.

3.2 Morphology analysis

Figure 5 displays the rupture side of the board of composite fibers subjected to different treatments, revealing noticeable changes in their surface morphology. The white arrow highlights evidence of fiber pullout. Figure 5A appears rough and frayed, indicating an untreated or minimally treated fiber. Figure 5B shows a more compact structure, suggesting partial treatment, while Figure 5C exhibits a smoother and more refined surface, likely due to an optimized chemical or thermal treatment. Fibers treated with 5 wt% NaCl at the boiling point have a more orderly fracture shape compared to the untreated board. These macro-level observations align with the SEM images of the fracture surface in Figures 5D, 5E, and 5F. It reveals the fiber-matrix interfacial bonding under different treatment conditions. The fibers in Figure 5D (corresponding to 5A) appear loosely packed with visible pull-outs and fractures, suggesting weak adhesion between the fiber and matrix, likely from untreated or minimally treated fibers. Figure 5E (corresponding to 5B) shows a clear improvement in bonding. This is evidenced by increased matrix adhesion to the fiber surfaces and irregular fiber breakage, indicating reduced fiber pull-out. In contrast, Figure 5F (corresponding to 5C) exhibits the most compact and well-integrated structure. Here, signs of separation from the matrix are minimized, and the fiber-matrix interaction is strong. These characteristics suggest that the applied treatment method—likely NaCl treatment at higher temperatures—significantly enhanced composite integrity. Collectively, the differences between these microstructures underscore the critical role of proper fiber treatment in improving the mechanical performance of composite materials.

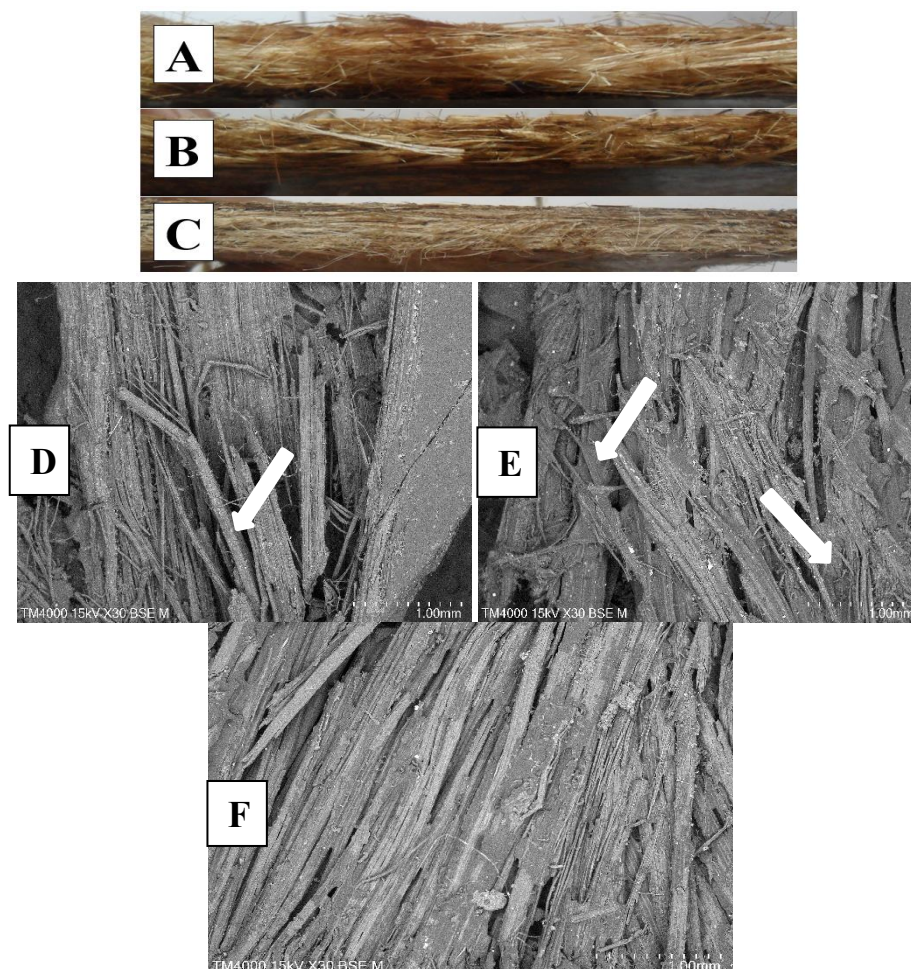


Figure 5. Surface of the composite boards using (A) untreated fiber, (B) 5 wt% NaCl at room temperature, (C) 5 wt% NaCl at boiling point at 0.80 g/cm^3 ; SEM morphology of (D) untreated fiber; (E) 5 wt% NaCl at room temperature; (F) 5 wt% NaCl at boiling temperature at 0.80 g/cm^3

This improvement is due to enhanced adhesion in the 5 wt% NaCl-treated composite board processed at the boiling point. Various chemical-treated methods reported in previous studies have demonstrated their effectiveness in strengthening adhesion between adhesives and biofibers [28]. Chemical treatments, crucial for enhancing adhesion between hydrophobic polymer adhesives and hydrophilic biofibers at the interface [12], [24] creates numerous pores on the fiber surface. These pores facilitate mechanical bonding while functional groups from the reagents (e.g., in sisal fiber modification) bind to hydroxyl groups in the fibers. The dual mechanism improves interfacial compatibility and bonding strength.

3.3 FTIR analysis

The FTIR spectra for both untreated and NaCl-treated sisal fibers are exhibited in Figure 6. The transmission band at 3330 cm^{-1} is linked to the O–H stretching vibration of the hydroxyl groups in the hydrogen-bonded fibers [31]. The intensity change of the O–H band at $\sim 3330 \text{ cm}^{-1}$ in sisal fiber after NaCl treatment (at room temperature and 100°C) is due to altered hydrogen bonding on the fiber surface. Na^+ and Cl^- ions disrupt or reorganize these bonds, especially at higher temperatures, reducing water content and changing cellulose structure. This affects the fiber's hydrophilicity and surface chemistry, as supported by recent studies [32]. The peak at approximately 2890 cm^{-1} is related to the C–H stretching vibration in the cellulose fibers [33],

band at 1736 cm^{-1} is correlated to the stretching of C–O bonds from aldehyde groups in the hemicellulose [34] and the band at 1635 cm^{-1} points to the aromatic characteristics of lignin [35]. Additional peaks at 1427 , 1340 , 1159 , and 1031 cm^{-1} are associated with C–O absorbed water in fibres [36] and O–H vibration [37], stretching of C–O–C of cellulose [38] and C–OH stretching in cellulose fibers [39], respectively.

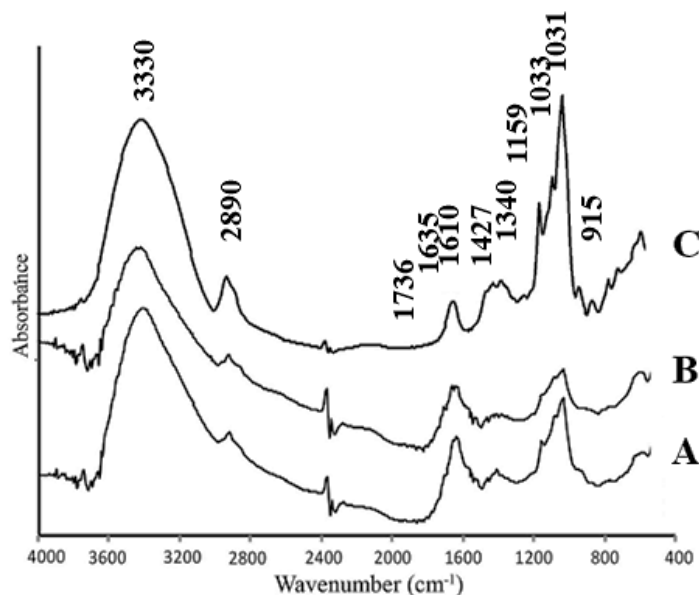


Figure 6. FTIR pattern of the composite boards using (A) untreated fiber, (B) 5 wt% NaCl at room temperature, and (C) 5 wt% NaCl at boiling point with density 0.80 g/cm^3

Following NaCl treatment, the reduction in intensity of the 1635 cm^{-1} band suggests a decrease in lignin content [27]. This band is also associated with O–H vibrations, corresponding to hydrogen-bonded water, which influences sample hydrophilicity [32]. Indeed, NaCl treatment modulates sample hydrophilicity, as increasing concentration can disrupt water structure near the surface, potentially enhancing hydrophobicity. This aligns with studies showing Na^+ and Cl^- ions affect interfacial water dynamics and surface properties [40]. Furthermore, new peaks at 915 cm^{-1} and 1610 cm^{-1} , associated with epoxide ring stretching vibrations [12], [41]. A clear peak at 1033 cm^{-1} , assigned to C–O and C–OH stretching in cellulose [42] emerge. The treatment modifies the fiber surface by ionic interactions, particularly Na^+ adsorption onto hydroxyl (–OH) and carboxyl (– COO^-) groups. This interaction alters fiber polarity, enhances adhesive compatibility, and promotes new polar functional groups (e.g., epoxy, – COO^-). These changes strengthen interfacial bonding, ultimately improving the composite board's overall properties.

3.4 Water absorption and swelling analysis

NaCl treatment of sisal fibers significantly reduced WA and TS after 24 hours of immersion. The TS of treated sisal composite boards was $2.13\text{--}4.22\%$, compliant with the $\leq 12\%$ limit of JIS A 5908 (Figure 7). NaCl treatment reduced TS by 48.14% (from 5.21% to 2.13%) at 0.80 g/cm^3 , 42.32% (from 4.63% to 2.67%) at 0.60 g/cm^3 , and 47.92% (from 4.09% to 2.13%) at 0.40 g/cm^3 compared to untreated composites.

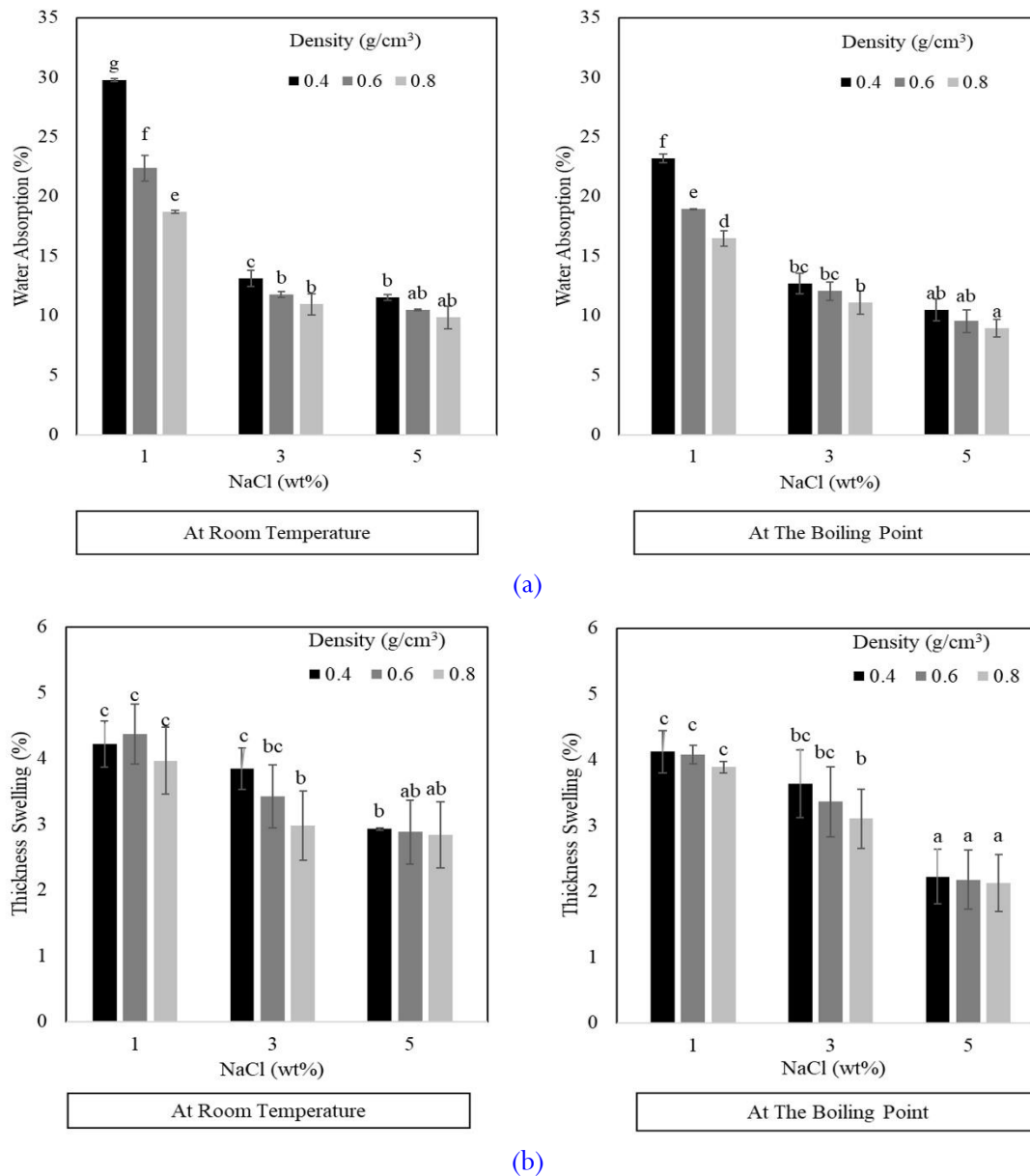


Figure 7. Response to moisture exposure of NaCl-treated sisal fiber-epoxy composite board: (A) TS and (B) WA

These results confirm that NaCl treatment significantly enhances the dimensional stability of sisal fiber composites by reducing thickness swelling (TS) and improving resistance to moisture-induced deformation compared to untreated boards. Increased NaCl concentration and immersion duration further optimized these properties. The enhanced dimensional stability stems from improved fiber-resin integration, where treatment promotes stronger interfacial adhesion and compatibility. This effectively counteracts swelling mechanisms triggered by water molecules penetrating the interface [43]. Moisture resistance has also been documented in NaOH-treated *Sesbania grandiflora* and Sisal fibers, showing reductions in moisture content of up to 30% [44],[45].

Water absorption compromises composite boards by swelling fibers, degrading mechanical properties, accelerating biodegradation, and inducing dimensional instability. Water infiltrates the composite through three primary mechanisms. The first mechanism involves the diffusion of water molecules into micro-gaps and voids within the composite structure. Second, water enters via capillary action through interfacial gaps and voids that result from incomplete fiber wettability and resin impregnation. Third, microcracks penetration, where flaws in the adhesive matrix promote

water ingress. The capillary mechanism is particularly critical, as it transports water to the fiber-adhesive interface. This process intensifies with weakened interfacial adhesion, ultimately causing fiber detachment. In NaCl-treated sisal composite boards, water absorption decreases significantly with higher immersion temperatures and NaCl concentrations. This reduction stems from Na^+ ions binding to hydroxyl ($-\text{OH}$) groups on the fiber's impurity-rich outer layer [20].

4. Conclusion

NaCl treatment improved fiber-matrix adhesion, thus enhancing the properties of sisal fiber-epoxy composite boards. It significantly increased MOE, MOR, and IB, while decreasing TS and WA. Optimal parameters (5 wt% of NaCl concentration, boiling point $\pm 100^\circ\text{C}$, density of 0.80 g/cm^3) yielded MOE of $4.59 \pm 0.26\text{ GPa}$, MOR of $18.88 \pm 0.03\text{ MPa}$, IB of $3.92 \pm 0.18\text{ MPa}$, TS of $2.13 \pm 0.43\%$, and WA of $8.95 \pm 0.05\%$. The treatment led to substantial improvements in mechanical strength, with MOE increasing by 130.65%, MOR increasing by 200.32%, and IB increasing by 218.70%. Additionally, the treatment enhanced dimensional stability, as indicated by a 48.14% reduction in thickness swelling and a 32.25% reduction in water absorption. The optimal results were achieved at 5 wt% NaCl concentration, a boiling point of 100°C , and a density of 0.80 g/cm^3 . These treatments highlight that NaCl has potential as an eco-friendly and cost-effective alternative to conventional chemical modifiers. This study contributed to a sustainable alternative for lightweight structural applications, reducing dependency on synthetic fiber composites. However, the study focused on small-scale laboratory fabrication, and further validation is required for the long-term stability of NaCl-treated fibers and large-scale production feasibility. Future studies should investigate the extent to which partial degradation of hemicellulose or surface roughening of fibers induced by NaCl treatment contributes to the enhancement of interfacial bonding. In addition, comparative analyses focusing on the mechanistic differences between NaCl and conventional chemical treatments, such as NaOH, are necessary to delineate the specific modifications imparted by each method on the fiber structure. Furthermore, molecular-level characterization employing advanced spectroscopic and microscopic techniques are warranted to elucidate the fiber-matrix interfacial interactions. It can provide detailed insights into the structural alterations of fiber constituents resulting from salt-based treatment processes.

Author's declaration

Author contribution

The authors confirm their contributions to the paper as follows: **Tamaryska Setyayunita**, contributed to the study conception and design. **Heru Suryanto** as a granted receiver, conducted the preparation of materials, data analysis and wrote the main manuscript. **Aminnudin Aminnudin** responsible for data collection and analysis; **Azlin Fazlina Osman** has an activity to review the manuscript and make revisions. **Uun Yanuhar** is responsible for data collection and analysis, and draft manuscript preparation: All authors reviewed the results and approved the final version of the manuscript.

Funding statement

This study received a grant from Universitas Negeri Malang for the Thesis Publication grant with contract no. 24.2.567/UN32.14.1/LT/2025.

Data Availability

The raw data of this study is available. If anyone wishes to use it as a basis for further research, please contact the corresponding author.

Acknowledgements

We would like to take this opportunity to express our heartfelt gratitude to Fajar Nusantara and Aldin for their help with administration in the laboratory.

Competing interest

The authors declare that they have no conflicts of interest to report regarding the present study.

Ethical clearance

This research does not involve humans as subjects.

AI statement

This article is the original work of the author without using AI tools for writing sentences and/or creating/editing tables and figures in this manuscript.

Publisher's and Journal's note

Universitas Negeri Padang as the publisher, and Editor of Teknomekanik state that there is no conflict of interest towards this article publication.

References

- [1] S. Cai *et al.*, "Review of synthetic polymer-based thermal insulation materials in construction and building," *Journal of Building Engineering*, vol. 97, p. 110846, 2024, <https://doi.org/10.1016/j.jobbe.2024.110846>
- [2] D. Sheng, R. Ma, and C. Su, "Static and Modal Analysis of a Box Structured Satellite Deployment Mechanism with self-actuated Torsion Joint," *Journal of Mechanical Engineering Science and Technology (JMEST)*, vol. 8, no. 1, p. 27, Mar. 2024, <https://doi.org/10.17977/um016v8i12024p027>
- [3] S. Islam, F.-E.- Karim, Md. R. Islam, Md. A. Saeed, K. A. Alam, and Mst. M. Khatun, "Thermoset and thermoplastic polymer composite with date palm fiber and its behavior: A review," *SPE Polymers*, vol. 6, no. 1, p. e10157, Jan. 2025, <https://doi.org/10.1002/pls2.10157>
- [4] W. Wirawan, H. I. Firmansyah, S. Adiwidodo, and M. S. Mustapa, "Impact of Print Speed and Nozzle Temperature on Tensile Strength of 3D Printed ABS for Permanent Magnet Turbine Systems," *Journal of Mechanical Engineering Science and Technology (JMEST)*, vol. 9, no. 1, pp. 90–102, 2025, <https://doi.org/10.17977/um016v9i12025p090>
- [5] S.-C. Shi, S.-W. Ouyang, and D. Rahmadiawan, "Erythrosine–Dialdehyde Cellulose Nanocrystal Coatings for Antibacterial Paper Packaging," *Polymers (Basel)*, vol. 16, no. 7, 2024, <https://doi.org/10.3390/polym16070960>
- [6] S.-C. Shi, S.-T. Cheng, and D. Rahmadiawan, "Developing biomimetic PVA/PAA hydrogels with cellulose nanocrystals inspired by tree frog structures for superior wearable sensor functionality," *Sens Actuators A Phys*, vol. 379, p. 115981, 2024, <https://doi.org/10.1016/j.sna.2024.115981>
- [7] S. Maiti, M. R. Islam, M. A. Uddin, S. Afroj, S. J. Eichhorn, and N. Karim, "Sustainable fiber-reinforced composites: A review," *Adv Sustain Syst*, vol. 6, no. 11, pp. 1–33, Nov. 2022, <https://doi.org/10.1002/adsu.202200258>
- [8] I. Elfaleh *et al.*, "A comprehensive review of natural fibers and their composites: An eco-friendly alternative to conventional materials," *Results in Engineering*, vol. 19, p. 101271, 2023, <https://doi.org/10.1016/j.rineng.2023.101271>

- [9] W. Qu, B. Niu, C. Lv, and J. Liu, "A Review of Sisal fiber-reinforced geopolymers: Preparation, microstructure, and mechanical properties," *Molecules*, vol. 29, no. 10, 2024, <https://doi.org/10.3390/molecules29102401>
- [10] A. M. Seid and S. A. Adimass, "Review on the impact behavior of natural fiber epoxy based composites," *Heliyon*, vol. 10, no. 20, p. e39116, 2024, <https://doi.org/https://doi.org/10.1016/j.heliyon.2024.e39116>
- [11] S. W. Ghorri and G. S. Rao, "Fiber loading of date palm and Kenaf reinforced epoxy composites: Tensile, impact and morphological properties," *J Renew Mater*, vol. 9, no. 7, pp. 1283–1292, 2021, <https://doi.org/10.32604/jrm.2021.014987>
- [12] T. Kanthiya *et al.*, "Modified Poly(Lactic Acid) epoxy resin using chitosan for reactive blending with epoxidized natural rubber: Analysis of annealing time," *Polymers (Basel)*, vol. 14, no. 6, p. 1085, Mar. 2022, <https://doi.org/10.3390/polym14061085>
- [13] S. Rao, M. Madhushree, and K. S. Bhat, "Characteristics of surface modified sugarcane bagasse cellulose: application of esterification and oxidation reactions," *Sci Rep*, vol. 14, no. 1, p. 24136, 2024, <https://doi.org/10.1038/s41598-024-75846-8>
- [14] S. Ullah, Z. Akhter, A. Palevicius, and G. Janusas, "Review: Natural fiber-based biocomposites for potential advanced automotive applications," *J Eng Fiber Fabr*, vol. 20, p. 15589250241311468, Jan. 2025, <https://doi.org/10.1177/15589250241311468>
- [15] H. Suryanto, S. Sukarni, Y. Rohmat, A. Pradana, U. Yanuhar, and K. Witono, "Effect of mercerization on properties of mendong (*Fimbristylis globulosa*) fiber," *Songklanakarin J. Sci. Technol.*, vol. 41, pp. 624–630, 2019, <https://www.thaiscience.info/Journals/Article/SONG/10993196.pdf>
- [16] M. Mohammed *et al.*, "Surface treatment to improve water repellence and compatibility of natural fiber with polymer matrix: Recent advancement," *Polym Test*, vol. 115, p. 107707, 2022, <https://doi.org/10.1016/j.polymertesting.2022.107707>
- [17] S. Rao, M. Madhushree, and K. S. Bhat, "Characteristics of surface modified sugarcane bagasse cellulose: application of esterification and oxidation reactions," *Sci Rep*, vol. 14, no. 1, p. 24136, 2024, <https://doi.org/10.1038/s41598-024-75846-8>
- [18] I. N. Santhiarsa, I. G. B. W. Kusuma, and I. G. A. Negara, "Mechanical characterization of NaOH-treated Agel fiber-Cotton composites," *Journal of Mechanical Engineering Science and Technology (JMEST)*, vol. 7, no. 2, p. 214, Nov. 2023, <https://doi.org/10.17977/um016v7i22023p214>
- [19] C. S. Wiguna, H. Suryanto, M. R. Fahlevi, J. Maulana, and U. Yanuhar, "Evaluation of Silane coupling agent treatment on Sansevieria cylindrica fiber as reinforcement in epoxy composite," *Journal of Engineering Science and Technology Review*, vol. 16, no. 4, pp. 41–46, 2023, <https://doi.org/10.25103/jestr.164.06>
- [20] M. H. Hamidon, M. T. H. Sultan, A. H. Ariffin, and A. U. M. Shah, "Effects of fibre treatment on mechanical properties of kenaf fibre reinforced composites: a review," *Journal of Materials Research and Technology*, vol. 8, no. 3, pp. 3327–3337, 2019, <https://doi.org/10.1016/j.jmrt.2019.04.012>
- [21] T. Setyayunita, H. Suryanto, and A. Aminnudin, "The influence of Sodium Chloride treatment on the Sisal fiber bundle's properties," *Journal of Mechanical Engineering Science and Technology (JMEST)*, vol. 8, no. 2, p. 532, Nov. 2024, <https://doi.org/10.17977/um016v8i22024p532>
- [22] U. S. Gupta *et al.*, "Plasma modification of natural fiber: A review," *Mater Today Proc*, vol. 43, pp. 451–457, 2021, <https://doi.org/10.1016/j.matpr.2020.11.973>
- [23] A. L. Andrady *et al.*, "Effects of UV radiation on natural and synthetic materials," *Photochemical & Photobiological Sciences*, vol. 22, no. 5, pp. 1177–1202, 2023, <https://doi.org/10.1007/s43630-023-00377-6>
- [24] T. Setyayunita, R. Widyorini, S. N. Marsoem, and D. Irawati, "Effect of different conditions of sodium chloride treatment on the characteristics of Kenaf fiber-epoxy composite board,"

- Journal of the Korean Wood Science and Technology*, vol. 50, no. 2, pp. 93–103, Mar. 2022, <https://doi.org/10.5658/WOOD.2022.50.2.93>
- [25] T. Setyayunita, R. Widyorini, S. N. Marsoem, and D. Irawati, “Study on the characteristics of NaCl treated Kenaf fiber epoxy composite board,” *IOP Conf Ser Earth Environ Sci*, vol. 891, no. 1, p. 012006, 2021, <https://doi.org/10.1088/1755-1315/891/1/012006>
 - [26] Japanese Standard Association, “Japanese Industrial Standard for Particleboard: JIS A 5908,” *Japanese Standard Association, Tokyo, Japan*, 2003.
 - [27] W. P. Raharjo, D. Ariawan, K. Diharjo, W. W. Raharjo, and B. Kusharjanta, “Effect of alkaline treatment time of fibers and microcrystalline cellulose addition on mechanical properties of unsaturated polyester composites reinforced by cantala fibers,” *Review on Advanced Materials Science*, vol. 62, no. 1, p. 20230103, 2023, <https://doi.org/10.1515/rams-2023-0103>
 - [28] H. Mardin, I. N. G. Wardana, Pratikto, W. Suprpto, and K. Kamil, “Effect of sugar palm fiber surface on interfacial bonding with natural Sago matrix,” *Advances in Materials Science and Engineering*, vol. 2016, no. 1, p. 9240416, Jan. 2016, <https://doi.org/10.1155/2016/9240416>
 - [29] T. Kanthiya *et al.*, “Modified Poly(Lactic Acid) Epoxy Resin Using Chitosan for Reactive Blending with Epoxidized Natural Rubber: Analysis of Annealing Time,” *Polymers (Basel)*, vol. 14, no. 6, p. 1085, Mar. 2022, <https://doi.org/10.3390/polym14061085>
 - [30] M. J. P. Macedo, G. S. Silva, M. C. Feitor, T. H. C. Costa, E. N. Ito, and J. D. D. Melo, “Surface modification of kapok fibers by cold plasma surface treatment,” *Journal of Materials Research and Technology*, vol. 9, no. 2, pp. 2467–2476, Mar. 2020, <https://doi.org/10.1016/j.jmrt.2019.12.077>
 - [31] M. Chandrasekar, M. R. Ishak, S. M. Sapuan, Z. Leman, and M. Jawaid, “A review on the characterisation of natural fibres and their composites after alkali treatment and water absorption,” *Plastics, Rubber and Composites*, vol. 46, no. 3, pp. 119–136, Mar. 2017, <https://doi.org/10.1080/14658011.2017.1298550>
 - [32] D. Rahmadiawan *et al.*, “Enhanced properties of TEMPO-oxidized bacterial cellulose films via eco-friendly non-pressurized hot water vapor treatment for sustainable and smart food packaging,” *RSC Adv*, vol. 14, no. 40, pp. 29624–29635, 2024, <https://doi.org/10.1039/D4RA06099G>
 - [33] A. Kodsangma *et al.*, “Effect of sodium benzoate and chlorhexidine gluconate on a bio-thermoplastic elastomer made from thermoplastic starch-chitosan blended with epoxidized natural rubber,” *Carbohydr Polym*, vol. 242, p. 116421, Aug. 2020, <https://doi.org/10.1016/j.carbpol.2020.116421>
 - [34] L. Nurhayati *et al.*, “Eco-friendly nanocellulose from coconut Fiber: Optimizing cellulase enzymes for sustainable production,” *Asian Journal of Green Chemistry*, vol. 9, no. 1, pp. 115–128, Feb. 2025, <https://doi.org/10.48309/AJGC.2025.482498.1559>
 - [35] H. Sukmana *et al.*, “Hungarian and Indonesian rice husk as bioadsorbents for binary biosorption of cationic dyes from aqueous solutions: A factorial design analysis,” *Heliyon*, vol. 9, no. 6, p. e17154, Jun. 2023, <https://doi.org/10.1016/j.heliyon.2023.e17154>
 - [36] R. Deepa, K. Kumaresan, and K. Saravanan, “Effect of surface chemical treatment of Himalayan Nettle and investigation of surface, physical and mechanical characteristics in treated Nettle fibre,” *Archives of Metallurgy and Materials*, vol. 68, no. No 2, pp. 571–578, 2023, <https://doi.org/10.24425/amm.2023.142436>
 - [37] Y. Xue *et al.*, “Strength enhancement of regenerated cellulose fibers by adjustment of hydrogen bond distribution in ionic liquid,” *Polymers (Basel)*, vol. 14, no. 10, p. 2030, May 2022, <https://doi.org/10.3390/polym14102030>
 - [38] L. R. F. Figueiredo, N. C. Nepomuceno, J. D. D. Melo, and E. S. Medeiros, “Glycerol-based polymer adhesives reinforced with cellulose nanocrystals,” *Int J Adhes Adhes*, vol. 110, p. 102935, 2021, <https://doi.org/10.1016/j.ijadhadh.2021.102935>

- [39] G. Paladini, V. Venuti, V. Crupi, D. Majolino, A. Fiorati, and C. Punta, "2D correlation spectroscopy (2D CoS) analysis of temperature-dependent FTIR-ATR spectra in branched Polyethyleneimine/TEMPO-oxidized cellulose nano-fiber xerogels," *Polymers (Basel)*, vol. 13, no. 4, 2021, <https://doi.org/10.3390/polym13040528>
- [40] F. Jiménez-Ángeles and A. Firoozabadi, "Hydrophobic Hydration and the Effect of NaCl Salt in the Adsorption of Hydrocarbons and Surfactants on Clathrate Hydrates," *ACS Cent Sci*, vol. 4, no. 7, pp. 820–831, Jul. 2018, <https://doi.org/10.1021/acscentsci.8b00076>
- [41] S. Zaidi, S. Thakur, D. Sanchez-Rodriguez, R. Verdejo, J. Farjas, and J. Costa, "Optimal processing conditions of a bio-based epoxy synthesized from vanillyl alcohol," *Polym Degrad Stab*, vol. 223, p. 110743, 2024, <https://doi.org/10.1016/j.polymdegradstab.2024.110743>
- [42] K. Kiattipornpithak *et al.*, "Reaction mechanism and mechanical property improvement of Poly(Lactic Acid) reactive blending with epoxy resin," *Polymers (Basel)*, vol. 13, no. 15, p. 2429, Jul. 2021, <https://doi.org/10.3390/polym13152429>
- [43] M. Mohammed *et al.*, "Challenges and advancement in water absorption of natural fiber-reinforced polymer composites," *Polym Test*, vol. 124, p. 108083, 2023, <https://doi.org/10.1016/j.polymertesting.2023.108083>
- [44] N. H. Sari, S. Suteja, and Y. A. Sutaryono, "The chemical and water sorption properties of chemically modified Sesbania grandiflora and Leucaena leucocephala fibers and their opportunities as biocomposite fillers," *Journal of Fibers and Polymer Composites*, vol. 3, no. 1, pp. 62–73, Mar. 2024, <https://doi.org/10.55043/jfpc.v3i1.146>
- [45] A. E. Bekele, H. G. Lemu, and M. G. Jiru, "Experimental study of physical, chemical and mechanical properties of enset and sisal fibers," *Polym Test*, vol. 106, p. 107453, 2022, <https://doi.org/10.1016/j.polymertesting.2021.107453>

Nomenclature

°C	: Degree Celcius	MPa	: Mega Pascal
ANOVA	: Analysis of Variance	MOE	: Modulus of Elasticity
FTIR	: Fourier Transform Infrared	MOR	: Modulus of Rupture
g/cm ³	: Gram per Centimeter Cubic	NaCl	: Sodium Chloride
g/g	: Gram per Gram	NaOH	: Sodium Hydroxide
GPa	: Giga Pascal	SEM	: Scanning Electron Microscope
IB	: Internal Bonding Strength	TS	: Thickness Swelling
JIS	: Japan Industrial Standard	w/w	: Weight per Weight
KBr	: Potassium Bromide	wt%	: Percent Weight
mm	: Millimeter	WA	: Water Absorption